

A Semi-empirical Model for Polarimetric Radar Backscattering from Bare Soil Surfaces

Yi-Sok Oh

Department of Radio Science and Communication Engineering, Hong-Ik University.

Abstract : A semi-empirical polarimetric backscattering model for bare soil surfaces is presented. Based on measurements by using polarimetric scatterometers and the JPL AirSAR, as well as the theoretical models, the backscattering coefficients σ_{vv}^0 , σ_{hh}^0 and σ_{vh}^0 , and the parameters of the co-polarized phase-difference probability density function, namely the degree of correlation α and the co-polarized-phase-difference ζ , are modeled empirically in terms of the volumetric soil moisture content m_v and the surface roughness parameters k_s and k_l , where $k=2\pi f/c$, s is the rms height and l is the correlation length.

Key Words : Polarimetric Radar Backscattering, Semi-empirical Model, AirSAR

1. Introduction

The small perturbation method (SPM), the physical optics (PO) model, the geometrical optics (GO) model(Ulaby *et al.*, 1982) and the integral equation method (IEM)(Fung and Chen, 1992; Fung, 1994) are commonly used for predicting the backscattering coefficients of rough surfaces. Empirical models based on polarimetric measurements have also been reported(Oh *et al.*, 1992; Dubios *et al.*, 1995), but they have dealt with only the magnitude of the backscattering response; *i.e.*, the backscattering coefficients, σ_{vv}^0 , σ_{hh}^0 and σ_{vh}^0 . Experimental data acquired by coherent polarimetric SAR systems and by polarimetric scatterometer systems have shown

that the probability density function (PDF) of the co-polarized phase angle $\phi_c = \phi_{hh} - \phi_{vv}$ as well as the backscattering coefficients, are strongly dependent upon the incidence angle, the wavelength, the soil moisture content and surface roughness. In contrast, the cross-polarized phase angle $\phi_x = \phi_{vh} - \phi_{vv} = \phi_{hv} - \phi_{vv}$ is uniformly distributed over $[0, 2\pi]$, and therefore contains no target-specific information(Sarabandi *et al.*, 1991; Sarabandi, 1992; Ulaby *et al.*, 1992). The PDF of ϕ_c is characterized completely by two parameters, namely the degree of correlation α and the coherent-phase-difference ζ (Sarabandi, 1992).

Unlike the backscattering coefficient of bare soil surfaces, no models currently exist for the parameters α and ζ , even though many

experimental observations have been reported (Sarabandi *et al.*, 1991; Sarabandi, 1992; Ulaby *et al.*, 1992; Skriver *et al.*, 1999). The goal of this study is to develop empirical models for the parameters α and ζ , as well as improved models for σ_{vv}^0 , σ_{hh}^0 and σ_{vh}^0 thereby providing a complete model for all of the ensemble-averaged differential Mueller matrix elements.

2. Theoretical Background

The backscattering coefficient of a distributed target can be computed from the following polarization synthesis equation (Ulaby and Elachi, 1990):

$$\sigma_{rr}^0(\psi_r, \chi_r; \psi_t, \chi_t) = 4\pi \bar{A}^r \cdot \bar{Q} \bar{M}^0 \bar{A}^t \tag{1}$$

where ψ is the rotation angle, χ is the ellipticity angle of the polarization ellipse, \bar{A}^r and \bar{A}^t are the normalized modified Stokes vectors for the receiving and transmitting antennas. The term $\bar{Q} \bar{M}^0$ is the modified differential Stokes scattering operator (Ulaby and Elachi, 1990), and \bar{M}^0 is the ensemble-averaged differential Mueller matrix (Sarabandi *et al.*, 1992), which can be computed from

$$\bar{M}^0 = \begin{bmatrix} \langle |S_{vv}^0|^2 \rangle & \langle |S_{vh}^0|^2 \rangle & \langle \text{Re}(S_{vh}^{0*} S_{vv}^0) \rangle & \langle -\text{Im}(S_{vh}^{0*} S_{vv}^0) \rangle \\ \langle |S_{hv}^0|^2 \rangle & \langle |S_{hh}^0|^2 \rangle & \langle \text{Re}(S_{hh}^{0*} S_{hv}^0) \rangle & \langle -\text{Im}(S_{hh}^{0*} S_{hv}^0) \rangle \\ \langle 2 \text{Re}(S_{vv}^0 S_{hh}^{0*}) \rangle & \langle 2 \text{Re}(S_{vh}^0 S_{hh}^{0*}) \rangle & \langle \text{Re}(S_{vv}^0 S_{hh}^{0*} + S_{vh}^0 S_{hv}^{0*}) \rangle & \langle -\text{Im}(S_{vv}^0 S_{hh}^{0*} - S_{vh}^0 S_{hv}^{0*}) \rangle \\ \langle 2 \text{Im}(S_{vv}^0 S_{hv}^{0*}) \rangle & \langle 2 \text{Im}(S_{vh}^0 S_{hh}^{0*}) \rangle & \langle \text{Im}(S_{vv}^0 S_{hh}^{0*} + S_{vh}^0 S_{hv}^{0*}) \rangle & \langle \text{Re}(S_{vv}^0 S_{hh}^{0*} - S_{vh}^0 S_{hv}^{0*}) \rangle \end{bmatrix} \tag{2}$$

Analysis of polarimetric data for various types of distributed targets, such as soil surfaces, indicates that the correlation between the two co-polarized scattering amplitudes $S_{vv}^0 S_{hh}^{0*}$ is quite

significant, while that between the co- and cross-polarized scattering amplitudes $S_{hv}^0 S_{hh}^{0*}$, $S_{vv}^0 S_{vh}^{0*}$, $S_{vh}^0 S_{vv}^{0*}$ or $S_{vh}^0 S_{hh}^{0*}$ is very weak (Sarabandi *et al.*, 1991; Sarabandi, 1992; Ulaby *et al.*, 1992; Skriver *et al.*, 1999; Oliver and Quegan, 1998). According to the reciprocity relation, the cross-polarized scattering amplitudes are identical in the backscattering direction, namely $S_{vh}^0 = S_{hv}^{0*}$. Therefore, the differential Mueller matrix can be approximated as follows (Sarabandi, 1992; Ulaby *et al.*, 1992):

$$\bar{M}^0 = \begin{bmatrix} M_{11}^0 & M_{12}^0 & 0 & 0 \\ M_{21}^0 & M_{22}^0 & 0 & 0 \\ 0 & 0 & M_{33}^0 & M_{34}^0 \\ 0 & 0 & M_{43}^0 & M_{44}^0 \end{bmatrix} \tag{3}$$

where

$$M_{11}^0 = \langle |S_{vv}^0|^2 \rangle \tag{4a}$$

$$M_{22}^0 = \langle |S_{hh}^0|^2 \rangle \tag{4b}$$

$$M_{12}^0 = M_{21}^0 = \langle |S_{vh}^0|^2 \rangle \tag{4c}$$

$$M_{33}^0 = \langle \text{Re}(S_{vv}^0 S_{hh}^{0*}) \rangle + \langle |S_{vh}^0|^2 \rangle \tag{4d}$$

$$M_{44}^0 = \langle \text{Re}(S_{vv}^0 S_{hh}^{0*}) \rangle - \langle |S_{vh}^0|^2 \rangle \tag{4e}$$

$$M_{43}^0 = -M_{34}^0 = \langle \text{Im}(S_{vv}^0 S_{hh}^{0*}) \rangle \tag{4f}$$

The PDF of the co-polarized phase angle $\psi_c = \psi_{hh} - \psi_{vv}$ was derived in (Sarabandi, 1992) as follows:

$$f_{\Phi}(\phi_c) = \quad (5)$$

$$\frac{1-\alpha^2}{2\pi(1-X^2)} \left\{ 1 + \frac{X}{\sqrt{1-X^2}} \left[\frac{\pi}{2} + \tan^{-1} \left(\frac{X}{\sqrt{1-X^2}} \right) \right] \right\}$$

where $X = \alpha \cos(\phi_c - \zeta)$, the parameter α , referred to as the degree of correlation, is a measure of the width of the PDF, and the parameter ζ referred to as the mean value of the co-polarized-phase-difference (Sarabandi, 1992), is the value of ϕ_c at which the PDF is a maximum. These two parameters completely specify $f_{\Phi}(\phi_c)$. Fig. 1 shows plots of the PDF for two different values of α and ζ . The PDF is approximately Gaussian in shape with a circular nature over $[-180, 180]$. The degree of correlation α is directly related to the standard deviation of ϕ_c , σ_{ϕ_c} , and the co-polarized-phase-difference ζ is equivalent to the mean of ϕ_c , $\bar{\phi}_c$.

The ensemble-averaged terms of the co-polarized scattering amplitudes in the differential Mueller matrix elements were derived in (Sarabandi, 1992; Ulaby *et al.*, 1992) using the parameters α and ζ as follows:

$$\langle \text{Re}(S_{vv}^0 S_{hh}^{0*}) \rangle = \alpha \cos \zeta \sqrt{M_{11}^0 M_{22}^0} \quad (6a)$$

$$\langle \text{Im}(S_{vv}^0 S_{hh}^{0*}) \rangle = \alpha \sin \zeta \sqrt{M_{11}^0 M_{22}^0} \quad (6b)$$

The backscattering coefficients are related with the ensemble-averaged differential scattering matrix elements as follows:

$$\sigma_{pq}^0 = 4\pi \langle |S_{pq}^0|^2 \rangle, \quad (7)$$

where the subscripts pq means that q-polarized wave is incident and p-polarized wave is scattered.

Conversely, the ensemble-averaged differential Mueller matrix elements can be computed from the three backscattering coefficients σ_{vv}^0 , σ_{hh}^0 , σ_{vh}^0 and the two phase-difference parameters α , ζ as follows:

$$M_{11}^0 = \frac{1}{4\pi} \sigma_{vv}^0 \quad (8a)$$

$$M_{22}^0 = \frac{1}{4\pi} \sigma_{hh}^0 \quad (8b)$$

$$M_{12}^0 = M_{21}^0 = \frac{1}{4\pi} \sigma_{vh}^0 \quad (8c)$$

$$M_{33}^0 = \frac{1}{4\pi} \left(\alpha \cos \zeta \sqrt{\sigma_{vv}^0 \sigma_{hh}^0} + \sigma_{vh}^0 \right) \quad (8d)$$

$$M_{44}^0 = \frac{1}{4\pi} \left(\alpha \cos \zeta \sqrt{\sigma_{vv}^0 \sigma_{hh}^0} - \sigma_{vh}^0 \right) \quad (8e)$$

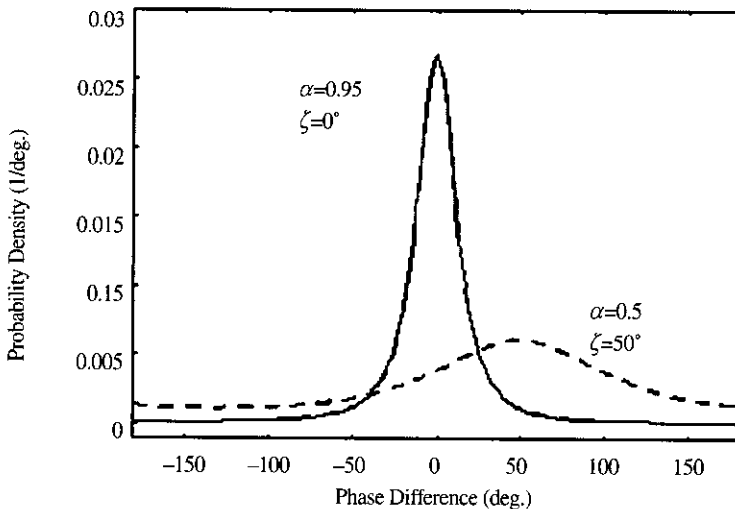


Fig. 1. Phase-difference PDFs with different values of α and ζ .

$$M_{43}^0 = M_{34}^0 = \frac{1}{4\pi} \sigma \sin \zeta \sqrt{\sigma_{vv}^0 \sigma_{hh}^0} \quad (8f)$$

3. Polarimetric Measurements

In support of the model development, an extensive database was generated of the *vv*-, *hh*-, and *vh*-polarized backscattering coefficients, the degree of correlation, and the co-polarized-phase-difference, obtained by a combination of ground-based scatterometers and the JPL airborne SAR system over a wide variety of bare soil surfaces. This database also includes precise ground truth data such as the surface roughness parameters and the volumetric soil moisture contents for all soil surfaces. Most of the soil surfaces were agricultural fields and their soil types were primarily silt loam, loam, or sandy loam. The database includes the following seven polarimetric measurements.

1) LCX POLARSCAT Data-1

This data set was obtained by a truck-mounted polarimetric scatterometer at 1.5 GHz, 4.75GHz and 9.5 GHz at the Botanical Garden of the University of Michigan in 1990(Oh *et al.*, 1992; Sarabandi *et al.*, 1991). Four different, random, bare soil fields were generated and each was measured under two different moisture conditions at incidence angles ranging from 10° to 70°(Oh *et al.*, 1992).

2) POLARSCAT Data-2

This data set was obtained by a truck-mounted polarimetric scatterometer at 1.25 GHz and 5.3 GHz during the cross-calibration experiment of the JPL AirSAR, and by a truck-mounted polarimetric scatterometer at Pellston, Michigan in 1991

(Sarabandi *et al.*, 1994). Three different rough soil fields were generated before the experiment and measured at incidence angles of 30°, 40° and 50°.

3) POLARSCAT Data-3

Four different soil surfaces were generated by flattening, tilling, raking and plowing four different agricultural fields located near Ypsilanti, Michigan. Then, the backscattering coefficients of these four fields were measured by a truck-mounted polarimetric scatterometer at 1.25 GHz, 5.3 GHz, and 9.6 GHz at incidence angles of 20°, 30°, 40°, 50°, 60°, and 70° over a period of two months. Table 1 provides a summary of the associated surface roughness and soil moisture conditions.

4) Polarimetric Scatterometer Data-4

An indoor polarimetric scatterometer system was used to measure the backscattering coefficients of two bare soil surfaces at 15 GHz at incidence angles ranging from 0° to 70° at Hong-Ik University, Seoul in 1999. The surface parameters measured for the first surface were *s*=0.45 cm, *l*=6.89 cm and *m_v*=0.09, and those for the second surface were *s*=0.40 cm, *l*=5.65 and *m_v*=0.19, where *s* is the rms height, *l* is the correlation length and *m_v* is the volumetric moisture content.

Table 1. Measured soil-surface parameters for POLARSCAT Data-3.

Surface Parameters	S-1	S-2	S-3	S-4	
rms height, <i>s</i> (cm)	0.55	0.94	1.78	3.47	
Correl. length, <i>l</i> (cm)	9.4	6.9	8.3	11.0	
Volumetric soil moisture content (top 3 cm layer)	M1	0.091	0.091	0.070	0.070
	M2	0.069	0.069	0.076	0.060
	M3	0.073	0.043	0.045	0.045
	M4	0.146	0.146	0.243	0.243
	M5	0.074	0.087	0.059	0.100
	M6	0.121	0.121	0.086	0.086
	M7	-	-	0.291	0.291
	M8	0.262	-	0.283	-

5) AirSAR Data-1

During the cross-calibration experiment involving the JPL AirSAR and a truck-mounted polarimetric scatterometer at Pellston, Michigan in 1991 (Sarabandi *et al.*, 1994), the backscatter responses at 1.25 GHz and 5.3 GHz were measured by the SAR at three different incidence angles (about 25°, 35° and 55°) for the same soil surfaces observed by the POLARSCAT Data-2.

6) AirSAR Data-2

During the Washita '92 experiment conducted at Chichasha, Oklahoma in 1992, the JPL AirSAR obtained backscatter data from various fallow fields for two weeks. Backscatter data for a large bare soil field (approximately 700m x 1400m) are available for various soil moisture conditions at 1.25 GHz and 5.3 GHz. The recorded soil surface parameters are $s = 1.82$ cm, $l = 17.75$ cm and $m_v = 0.287, 0.224, 0.241, 0.181, 0.136, 0.116$ at about 55° and $m_v = 0.241, 0.175$ at about 34°.

7) AirSAR Data-3

In 1993, the JPL AirSAR was used to measure the radar backscatter response of various agricultural fields near Davis, California. Backscatter and ground surface data were recorded for 19 bare soil fields at 1.25 GHz. The rms heights of those fields ranged from 0.61 cm to 2.5 cm, and the correlation lengths varied from 1.73 cm to 11.9 cm, and the volumetric moisture contents varied from 0.035 to 0.144.

4. Modeling Procedure

The input parameters for the intended polarimetric model include incidence angle θ , the volumetric soil moisture content m_v , and the

roughness parameters ks and kl , where s is the rms height, l is the correlation length and k is the wavenumber. Because the backscatter is only weakly dependent on soil type, in comparison with its response to surface roughness and soil moisture, the soil type has been excluded in this model. The soil moisture content m_v is used in the model instead of the complex dielectric constant for simplicity. Moreover, the soil moisture content of the top 3-cm soil-surface layer is used at all frequencies because it was shown that the top 2~3 cm soil layer exhibits the greatest influence on the radar backscatter response even though the wave may penetrate deeper into the soil for a dry surface at L-band (Oh, 2000).

1) vh -polarized Backscattering Coefficient

It was found that the cross-polarized backscattering coefficient of the semi-empirical model described in (Oh *et al.*, 1992) agrees very well with the measurements, especially with regard to its dependence on θ . The model expresses σ_{vh}^0 in terms of the Fresnel reflectivity (or indirectly through the complex dielectric constant), the incidence angle and the roughness parameter ks .

After examining the angular patterns of the measured data, the form of $(\cos\theta)^c$ is selected as a candidate function for characterizing the angular dependence, and $1 - \exp[-a ks^b]$ function is used to account for the response to surface roughness. This roughness function satisfies the conditions that the cross-polarized backscattering coefficient approaches zero for a smooth (near flat) surface ($ks \rightarrow 0$) and that on the other extreme it becomes independent of ks for a very rough surface ($ks \rightarrow \infty$). Hence, the proposed overall functional form for the cross-polarized backscattering coefficient is as follows:

$$\sigma_{vh}^0 = am_v^b (\cos \theta)^c [1 - \exp(-d(ks)^e)] \quad (9a)$$

The magnitudes of constants a , b , c , d and e were determined through data fitting, using the database, by applying the minimum mean square error (MMSE) technique. The process led to the following formula:

$$\sigma_{vh}^0 = 0.11m_v^{0.7} (\cos \theta)^{2.2} [1 - \exp(-0.32(ks)^{1.8})] \quad (9b)$$

Fig. 2 shows a comparison between our model and the IEM (Fung and Chen, 1992; Fung, 1994) for an incidence angle of 45° and a soil moisture content $m_v=0.13$. The figure also includes data measured at angles in the range $35^\circ < \theta < 55^\circ$ and for moisture in the range $0.03 < m_v < 0.3$. For the IEM computation, an approximate form for small-to-moderate ks ($ks < 3$) (Fung and Chen, 1992) with an exponential correlation function with $kl = ks/0.15$ was used. Our proposed model agrees well with the measurement across the entire range of ks , and agrees with the IEM for the range of $ks > 0.2$. For

surfaces with $ks < 0.2$, the IEM fails to match the observed data.

2) vv-polarized Backscattering Coefficient

The cross-polarized ratio q is defined as $q = \sigma_{vh}^0 / \sigma_{vv}^0$ as in (Oh *et al.*, 1992), where it is expressed as proportional to the term of $[1 - \exp[-ks]]$ and to $\sqrt{\Gamma_0}$. Analysis of the database shows that the measured values of q agree quite well with $c_1[1 - \exp[-ks]]$. Fig. 3 shows the measured values of q for $0.03 < m_v < 0.3$, $0.03 < s/l < 0.32$ at $29^\circ < \theta < 51^\circ$, compared with the functional form given by $a[1 - \exp[-0.9(ks)^{0.8}]]$. Also shown is a set of curves calculated on the basis of the IEM, assuming an exponential autocorrelation function with $m_v=0.15$, $\theta=40^\circ$, and three values of s/l .

Data analysis shows that the sensitivity of the measured q to incidence angle θ is high enough for modeling, while that to the soil moisture m_v is very weak. Based on the preceding analysis, a functional form was chosen for the cross-

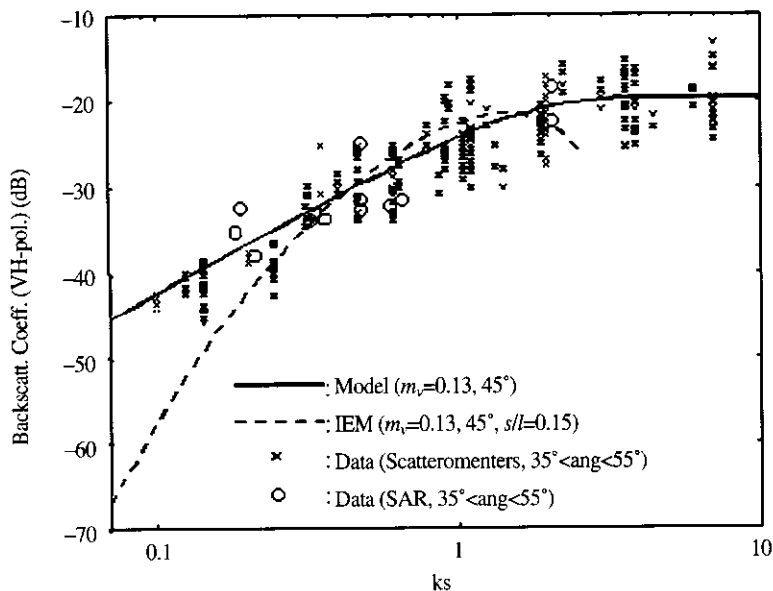


Fig. 2. Measurements of σ_{vh}^0 for conditions over the range of $35^\circ < \theta < 55^\circ$, $0.03 < m_v < 0.3$ and $0.03 < s/l < 0.32$. The measurements are compared with curves calculated using the IEM and the semi-empirical model, both for $\theta = 45^\circ$ and $m_v = 0.13$.

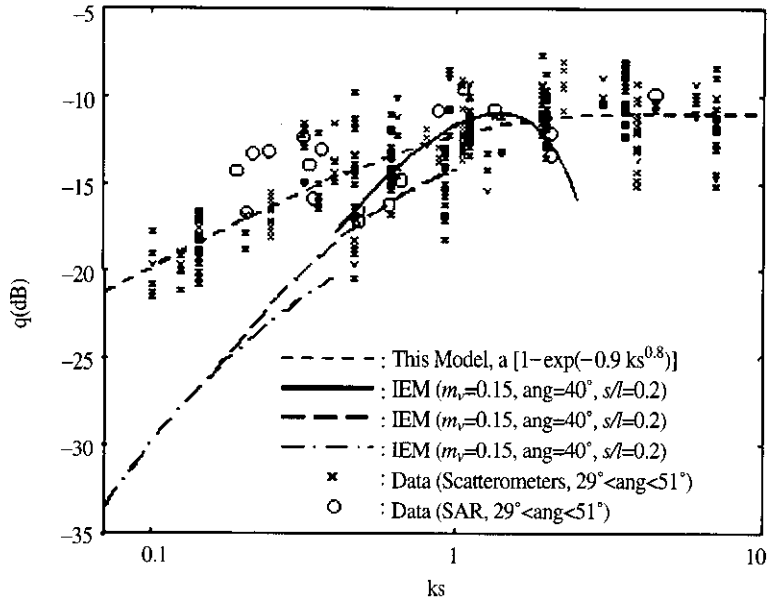


Fig. 3. Measured variation of the cross-polarized ratio $\sigma_{vh}^0/\sigma_{vv}^0$ with ks , where the measurements cover the range $29^\circ < \theta < 51^\circ$, $0.03 < m_v < 0.3$ and $0.03 < s/l < 0.32$. Curves calculated in accordance with the semi-empirical model and the IEM are shown for comparison.

polarized ratio, and the MMSE data-fit gives the following formula:

$$q = \sigma_{vh}^0/\sigma_{vv}^0 = 0.1(m = \sin 1.3\theta)^{1.2} \{1 - \exp[-0.9(ks)^{0.8}]\}, \quad (10)$$

where m is the surface slope, defined here as $m = s/l$.

Upon combining (9) and (10), the vv -polarized

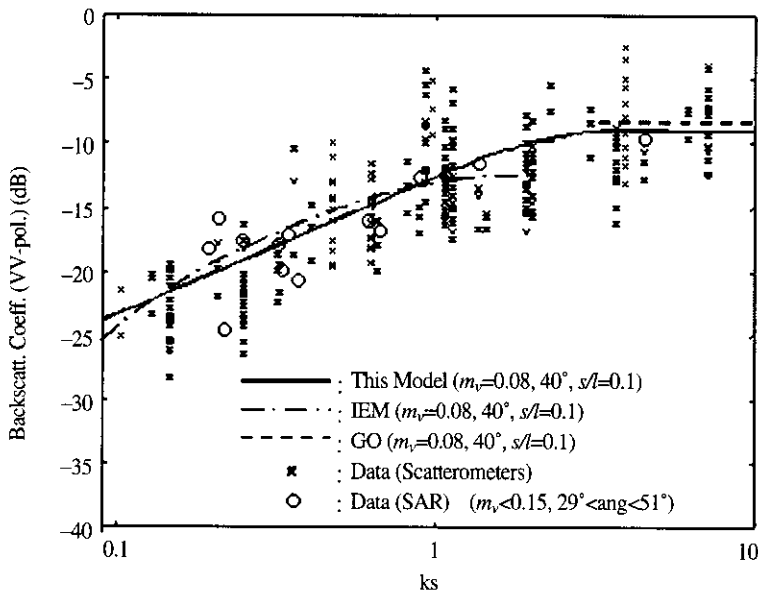


Fig. 4. Plots of σ_{vv}^0 , calculated in accordance with the IEM, the GO model, and the semi-empirical model, for $\theta = 40^\circ$, $m_v = 0.08$ and $s/l = 0.1$. Also included are measurements over the range $29^\circ < \theta < 51^\circ$, $0.03 < m_v < 0.15$ and $0.03 < s/l < 0.32$.

backscattering coefficient is obtained. Fig. 4 displays measured values of σ_{vv}^0 as a function of ks . Also shown is the semi-empirical model calculated for median conditions, as well as the IEM ($ks < 2$) and GO model ($ks > 3$). For the GO model computation, a surface correlation function $\rho(\xi) = [1 + \xi^2 / l^2]^{-1.5}$ was assumed (Ulaby *et al.*, 1982, Ch. 12). The empirical model agrees well with the measurements over the entire range of ks , and it also agrees with the IEM for $ks < 2$ and with the GO model for $ks > 3$.

3) *hh*-polarized Backscattering Coefficient

Next, the co-polarized ratio $p = \sigma_{hh}^0 / \sigma_{vv}^0$ is examined. The SPM, which is valid for small ks values, shows that the σ_{vv}^0 is higher than σ_{hh}^0 and that the ratio p depends on the dielectric constant (and therefore on the soil moisture content) and the incidence angle, while the GO model, which is valid for large ks values, shows that σ_{vv}^0 is always equal to σ_{hh}^0 . We know that $p = 1$ (0 dB) at normal incidence ($\theta = 0^\circ$) for any surface, and it is also equal to 1 when the surface is very rough ($ks \rightarrow \infty$) at any incidence angle. Incorporating these limiting cases with expectations on the variations of p with m_v and ks , the following form of p was obtained.

$$p \equiv \frac{\sigma_{hh}^0}{\sigma_{vv}^0} = 1 - \left(\frac{\theta}{90^\circ} \right)^{0.35 m_v^{-0.65}} \cdot e^{-0.4(ks)^{1.4}}, \quad (11)$$

where θ is the incidence angle in degrees.

Fig. 5(a) shows the variation of the measured p to ks for data over the range $0.03 < m_v < 0.3$ and $0^\circ < \theta < 70^\circ$. For comparison, model curves are shown for two extreme cases, namely $m_v = 0.03$ and $\theta = 10^\circ$, and $m_v = 0.3$ and $\theta = 70^\circ$, as well as curves based on the IEM for the same extreme cases. Fig. 5(b) shows the variation of the measured p to θ for data over the range

$0.03 < m_v < 0.3$ and $0.1 < ks < 7$, and again similar model comparisons are included. In both cases, the semi-empirical model provides better bounds than the IEM. We can compute the *hh*-polarized backscattering coefficient σ_{hh}^0 by simply combining (9), (10) and (11).

$$\sigma_{hh}^0 = p \sigma_{vv}^0 = \frac{p}{q} \sigma_{vh}^0.$$

4) Degree of Correlation

Up to the present, no model has been published containing explicit expressions for the statistical parameters of the phase-difference PDF, namely the degree of correlation α and the co-polarized-phase-difference ζ . Hence, our model effort will rely on polarimetric measurements of bare soil surfaces and on numerical computations of backscattering from one-dimensional inhomogeneous, dielectric, rough surfaces (Sarabandi *et al.*, 1996). For an isotropic homogeneous rough surface, there is no phase-difference between the *vv*- and *hh*-polarized backscattering amplitudes at $\theta = 0^\circ$. Therefore, the PDF of the phase-difference angle is a delta function at $\theta = 0^\circ$, which corresponds to $\alpha = 1$. The measurement database and the numerical computation show that α decreases as θ increases, and the angular variation of α depends strongly on the surface roughness and weakly on the soil moisture content.

After close examination of the database, the following functional form was chosen:

$$\alpha = 1 - A(\sin\theta)^B, \quad (12)$$

where A and B may depend on the surface roughness and soil moisture content. At first, A and B were determined for each of many subsets in the database, with each subset defined over a narrow range of the parameters m_v , ks , kl , and s/l . Then, functional forms were deployed and the MMSE

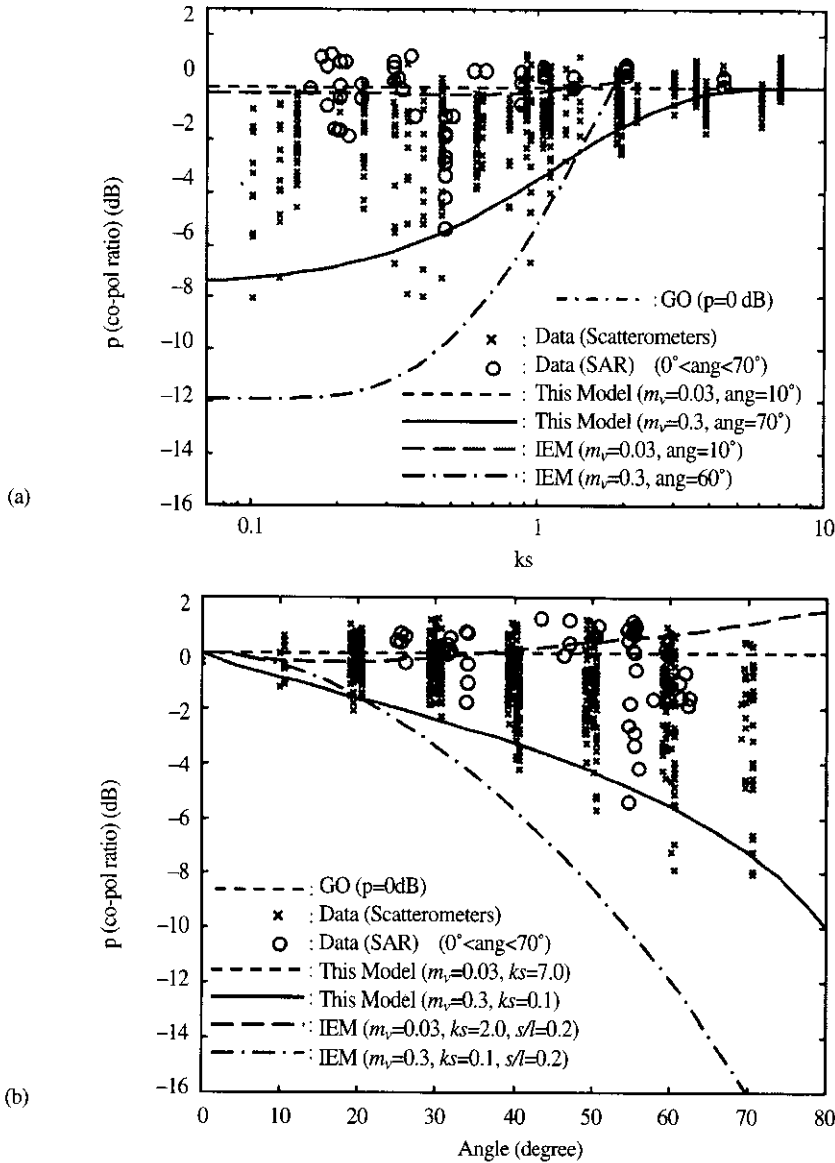


Fig. 5. Variation of the co-polarized ratio $\frac{\sigma_{HH}^0}{\sigma_{VV}^0}$ with (a) ks and (b) θ , for measurements over the range $0.03 < m_v < 0.3$ and $0^\circ < \theta < 70^\circ$. Curves calculated on the basis of the semi-empirical model, the IEM and the GO model, are shown for two relatively extreme surface conditions.

technique was applied for A and B , leading to:

$$\alpha = 1 - (0.17 + 0.001kl + 0.5m_v) \cdot (\sin\theta)^{1.1(ks)^{-0.4}} \quad (13)$$

Fig. 6 shows the variation of the measured α with θ for the range $0.03 < m_v < 0.3$, $0.1 < ks < 7$, and $1.8 < kl < 22$, and the two calculated curves

bounding the data represent two relatively extreme conditions.

5) Co-polarized-phase-difference

The co-polarized-phase-difference ζ is a measure of the mean value of the co-polarized

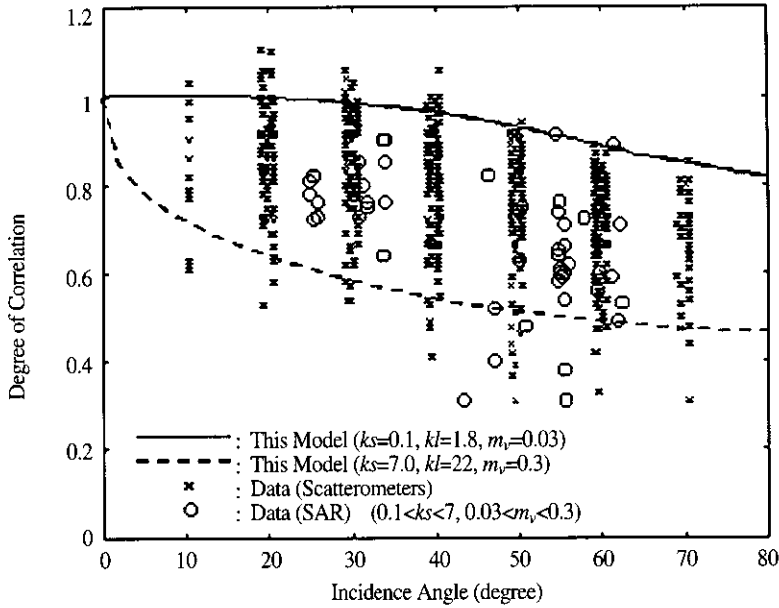


Fig. 6. Measured degree of correlation compared with model predictions for two relatively extreme surface conditions.

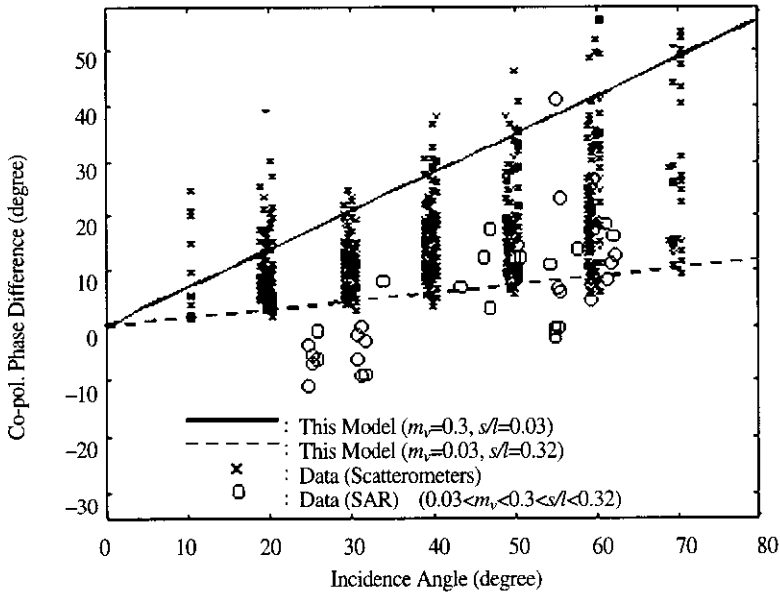


Fig. 7. Measured co-polarized-phase-difference compared with model predictions for two relatively extreme surface conditions.

phase angle ϕ_c . At $\theta=0^\circ$, ζ should be zero because there should be no phase-difference between the vv - and hh -polarized backscattering amplitudes for an isotropic surface. A data-fitting process similar

to that used in the preceding section led to the following formula:

$$\zeta = \left(0.44 - 0.95m_v - \frac{ks}{kl} \right) \theta, \quad (14)$$

where θ is the incidence angle in degrees. Fig. 7 shows the variation of the measured ζ to θ , and again the model captures the bulk of the data within the range represented by the two rather extreme conditions specified in the figure.

As shown in Figs. 6 and 7, the data measured by the AirSAR are lower than those measured by the polarimetric scatterometers. The phase-difference parameters measured by the polarimetric scatterometers are accurate because the data were calibrated by the differential Mueller matrix technique using the polarimetric response of a calibration target over the entire mainlobe of the scatterometer (Sarabandi *et al.*, 1992). When a traditional calibration technique for a distributed target is used, *i.e.* the differential Mueller matrix is approximated by the Mueller matrix divided simply by an illuminated area, the α and the ζ are inaccurate as shown in (Sarabandi *et al.*, 1992). For the scatterometer data, the α values obtained by the old illumination-integral calibration technique were about 0.8 times the α values determined by the new accurate differential Muller matrix calibration technique.

5. Verification

Calculations based on these expressions were compared with numerous subsets of the overall database. For most data sets, the model-calculated angular responses of σ_{vv}^0 , σ_{hh}^0 and σ_{vh}^0 are agreed very well with the measured data. The comparison between model calculations of respectively the degree of correlation α and the co-polarization phase angle ζ and measured data is also show a good agreement.

Further comparison between the model and measured data can be made in terms of the

Mueller matrix. At $\theta=30^\circ$, a surface with $ks=0.126$, $kl=2.62$ and $m_v=0.126$ was measured by the scatterometer to have a differential Mueller matrix:

$$\overline{M}_{meas} = \begin{bmatrix} 0.0012 & 0.0002 & 0.0000 & 0.0000 \\ 0.00002 & 0.0008 & 0.0000 & 0.0000 \\ 0.0000 & 0.0000 & 0.0010 & -0.0002 \\ 0.0000 & 0.0000 & 0.0002 & 0.0010 \end{bmatrix} \quad (15)$$

As described in Section 2, the differential Mueller matrix can be computed from σ_{vv}^0 , σ_{hh}^0 , σ_{vh}^0 , α and ζ each of which can be computed using the expressions provided by the semi-empirical polarimetric model in terms of the surface parameters. For the surface parameters associated with the measured matrix given in (15), such a process leads to:

$$\overline{M}_{comp} = \begin{bmatrix} 0.0012 & 0.0001 & 0.0000 & 0.0000 \\ 0.00001 & 0.0009 & 0.0000 & 0.0000 \\ 0.0000 & 0.0000 & 0.0009 & -0.0003 \\ 0.0000 & 0.0000 & 0.0003 & 0.0009 \end{bmatrix} \quad (16)$$

The corresponding elements of the two differential Mueller matrices are in very good agreement. Elements other than M_{11} , M_{22} , M_{33} , M_{34} , M_{43} and M_{44} of the differential Mueller matrix are negligible for radar backscattering from soil surfaces.

6. Concluding Remarks

A semi-empirical polarimetric backscattering model was developed for random bare soil surfaces using a combination of truck-mounted scatterometer measurements and airborne SAR observations, both supported by extensive ground observation of the soil surface statistics and moisture content. The functional form of the model was constrained to insure that its

predictions are consistent with known theoretical values, such as $\sigma_{vv}^0 = \sigma_{hh}^0$ at normal incidence, $\sigma_{vv}^0 / \sigma_{hh}^0$ for an electromagnetically very rough surface, and $\sigma_{vh}^0 / \sigma_{vv}^0$ approaches a constant as surface roughness exceeds $ks = 3$. The two distinguishing features of the model is that it not only agrees with experimental observations over a wide range of soil surface conditions, but it also agrees with the IEM and geometrical optics model over their individual regions of validity, thereby encompassing the full range of surface roughness encountered under natural conditions.

Acknowledgements:

Author thanks to Professor Fawwaz T. Ulaby for his review and his valuable comments.

References

- F.T. Ulaby, M.K. Moore, and A.K. Fung, 1982. *Microwave Remote Sensing, Active and Passive*, vol. 2, Artech House, Norwood, MA, U.S.A.
- A.K. Fung, Z. Li and K.S. Chen, 1992. Backscattering from a randomly rough dielectric surface, *IEEE Trans. Geosci. Remote Sensing*, 30: 356-369.
- A.K. Fung, 1994. *Microwave Scattering and Emission Models and Their Applications*, Artech House, Boston, MA.
- Y. Oh, K. Sarabandi and F.T. Ulaby, 1992. An empirical model and an inversion technique for radar scattering from bare soil surfaces, *IEEE Trans. Geosci. Remote Sensing*, 30: 370-382.
- P.C. Dubois, J. van Zyl and E.T. Engman, 1995. Measuring soil moisture with imaging radar, *IEEE Trans. Geosci. Remote Sensing*, 33: 916-926.
- K. Sarabandi, Y. Oh and F.T. Ulaby, 1991. Polarimetric radar measurement of bare soil surfaces at microwave frequencies, *Proc. of IEEE Geosci. Remote Sensing Symp., Espoo*.
- K. Sarabandi, 1992. Derivation of phase statistics of distributed targets from the Mueller matrix, *Radio Sci.*, 27: 553-560.
- F.T. Ulaby, K. Sarabandi, and A. Nashashibi, 1992. Statistical properties of the Mueller matrix of distributed targets, *IEE Proc.-F*, 139(2): 136-146.
- H. Skriver, M.T. Svendsen and A.G. Thompsen, 1999. Multitemporal C- and L-band polarimetric signatures of crops, *IEEE Trans. Geosci. Remote Sensing*, 37: 2413-2428.
- F.T. Ulaby and C. Elachi, 1990. *Radar Polarimetry for Geoscience Applications*, Artech House, Norwood, MA.
- K. Sarabandi, Y. Oh and F.T. Ulaby, 1992. Measurement and calibration of differential Mueller Matrix of distributed targets, *IEEE Trans. Antennas Propagat.*, 40: 1524-1532.
- C. Oliver and S. Quegan, 1998. *Understanding Synthetic Aperture Radar Images*, Artech House, Norwood, MA.
- K. Sarabandi, L. Pierce, Y. Oh, M.C. Dobson, F.T. Ulaby, A. Freeman, and P. Dubois, 1994. Cross-calibration experiment of JPL AIRSAR and Truck-mounted polarimetric scatterometer, *IEEE Trans. Geosci. Remote Sensing*, 32: 975-985.
- Y. Oh and Y.C. Kay, 1998. Condition for precise measurement of soil surface roughness, *IEEE Trans. Geosci. Remote Sensing*, 36: 691-695.

- Y. Oh, 2000. Retrieval of the Effective Soil Moisture Contents as a Ground Truth from Natural Soil Surfaces, in *Int. Geoscience and Remote Sensing Symp. (IGARSS2000)*.
- Y. Du, F.T. Ulaby and M.C. Dobson, 2000. Sensitivity to soil moisture by active and passive microwave sensors, *IEEE Trans. Geosci. Remote Sensing*, 38: 105-113.
- K. Sarabandi, Y. Oh, and F.T. Ulaby, 1996. A numerical simulation of scattering from one-dimensional inhomogeneous dielectric random surfaces, *IEEE Trans. Geosci. Remote Sensing*, 34(2): 425-432.